



HAL
open science

A COMPARISON OF THE REPRODUCIBILITY AND HOMOGENEITY OF AMORPHOUS Cu-Zr ALLOYS PREPARED BY ROLLER-QUENCHING AND MELT SPINNING

Y. Calvayrac, Mireille L. Harmelin-Vivien, A. Quivy, Jérôme Chevalier, J.
Bigot

► **To cite this version:**

Y. Calvayrac, Mireille L. Harmelin-Vivien, A. Quivy, Jérôme Chevalier, J. Bigot. A COMPARISON OF THE REPRODUCIBILITY AND HOMOGENEITY OF AMORPHOUS Cu-Zr ALLOYS PREPARED BY ROLLER-QUENCHING AND MELT SPINNING. *Journal de Physique Colloques*, 1980, 41 (C8), pp.C8-114-C8-117. 10.1051/jphyscol:1980830 . jpa-00220336

HAL Id: jpa-00220336

<https://hal.science/jpa-00220336>

Submitted on 4 Feb 2008

HAL is a multi-disciplinary open access archive for the deposit and dissemination of scientific research documents, whether they are published or not. The documents may come from teaching and research institutions in France or abroad, or from public or private research centers.

L'archive ouverte pluridisciplinaire **HAL**, est destinée au dépôt et à la diffusion de documents scientifiques de niveau recherche, publiés ou non, émanant des établissements d'enseignement et de recherche français ou étrangers, des laboratoires publics ou privés.

A COMPARISON OF THE REPRODUCIBILITY AND HOMOGENEITY OF AMORPHOUS Cu-Zr ALLOYS PREPARED BY ROLLER-QUENCHING AND MELT SPINNING

Y. Calvayrac, M. Harmelin, A. Quivy, J.P. Chevalier and J. Bigot

C.E.C.M.-C.N.R.S., 15, rue G. Urbain, 94400 Vitry, France

Introduction. Detailed studies have been devoted to the thermal stability of the $\text{Cu}_{60}\text{Zr}_{40}$ amorphous alloy (1,2,3). However there are some disagreements in these descriptions. As the amorphous state is not in thermodynamic equilibrium, the reason for these disagreements may lie in the preparation procedures : Differences in quenching rate, chemical homogeneity of the samples, contamination by the crucible or by the protective atmosphere, should produce differences in the glassy state which is obtained. This paper describes experimental comparisons of the thermal behaviour of $\text{Cu}_{60}\text{Zr}_{40}$ amorphous samples prepared by the two methods of twin-roll quenching and melt-spinning.

Experimental. The starting alloy ($\sim 50\text{g}$) is prepared from electrolytic copper and Kroll zirconium by levitation melting under a helium atmosphere. This ingot is then broken into small pieces ($\sim 3\text{g}$) which are melted again and twin-roll quenched or melt-spun. The twin-roll quench is performed under a helium atmosphere. For this method, levitation melting is used and prevents any contamination by a crucible. The amorphous foils are typically 20mm wide and 0.1 mm thick. The preparation by melt-spinning is generally performed in flowing helium. The alloy is melted in a silica tube. The amorphous ribbons are about 3mm wide, 0.05 mm thick and 3m long. Some ribbons have been prepared by melt-spinning in air but then oxygen is incorporated in the alloy and the thermal behaviour of the amorphous ribbons is modified.

The structure of the quenched foils is examined with a step-scan X-Ray diffractometer using Co K α radiation, and in some cases with transmission electron microscopy. DTA curves are recorded with a micro differential thermal analyser SETARAM under a 99.995 % argon gas atmosphere. The sample mass is about 15mg. The heating rate is $10 \text{ K} \cdot \text{min}^{-1}$.

Results.

Reproducibility of the as-quenched material.

Tables I and II give the crystallization temperature T_c , the heat of crystallization ΔH and the glass transition temperature T_g for a twin-roll thin foil and a melt-spun ribbon respectively. All samples were previously determined to have no trace of crystallinity by X-Ray diffraction. T_g and T_c are extrapolated temperatures : they are defined as the temperatures at which the extrapolated baseline intersects the steepest tangent to the peaks.

Table I.

T_g , T_c and ΔH for a $\text{Cu}_{60}\text{Zr}_{40}$ amorphous thin foil obtained by the twin-roll quenching technique. The different samples are cut from the same foil.

sample number	1	2	3	4	5	6	7
T_g (K)	702	703	701	701	701	701	703
T_c (K)	745	745	746	746	746	745	746
ΔH (kJ.mole ⁻¹)	3.9	4.1	4.4	4.3	4.0	4.1	4.1

Table II.

T_g , T_c and ΔH for a $\text{Cu}_{60}\text{Zr}_{40}$ amorphous ribbon prepared by melt-spinning in helium. The different samples are cut from the same ribbon, every 40 cm.

sample number	1	2	3	4	5
T_g (K)	700	699	702	702	701
T_c (K)	752	751	750	750	749
ΔH (kJ.mole ⁻¹)	4.2	4.1	4.3	4.2	3.9

It appears that, for the same twin-roll quenched foil or the same melt-spun ribbon, the scatter in the values of T_g , T_c and ΔH is smaller than the experimental accuracy ($\pm 3\text{K}$ for T_g and T_c , $\pm 6\%$ for ΔH).

Results show considerably more scatter if the samples are chosen in different ribbons, obtained by different quenches (Table III). Moreover a careful examination of DTA curves shows that the relative temperatures of the end of the glass

transition T_{gf} and the crystallization temperature T_c vary significantly from sample to sample. (T_{gf} is defined as the temperature at which the specific heat C_p attains its higher value).

Table III.
Thermal characteristics of different melt-spun ribbons.

Sample number	T_g (K)	T_{gf} (K)	$\Delta C_p \times 10^3$ (KJ.mole ⁻¹ .K ⁻¹)	T_c (K)	ΔH (kJ.mole ⁻¹)	$T_c - T_g$ (K)	$T_c - T_{gf}$ (K)
1	708	731	22	756	4.3	48	25
2	703	723	21	746	4.3	43	23
3	701	723	23	746	4.1	45	23
4	702	723	21	744	4.1	42	21
5	702	723	20	743	4.1	41	20
6	705	725	19	742	4.1	37	17
7	701	720	16	737	4.0	36	17
8	698	720	19	736	4.1	38	16
9	698	718	15	734	4.0	36	16
10	699	718	17	734	4.3	35	16

Along a given amorphous ribbon (i.e. for a given quench) the ($T_c - T_{gf}$) interval remains constant. Ten different ribbons have been prepared on the same day and immediately examined to prevent any difference in temperature-time history. On figure 1 the beginnings of their crystallization exotherms have been plotted taking T_{gf} as time origin: An increase in ($T_c - T_{gf}$) from sample 10 to sample 1 clearly appears. Table III shows that corresponding increases occur in ($T_c - T_g$) and T_g values. The thermal stability of glasses is often measured as the difference between T_c and T_g (4): More stable glasses have larger ($T_c - T_g$) values. The differences in thermal stability of the ten ribbons are confirmed by the results of isothermal annealing experiments near T_g : the volume fraction of crystalline material formed on annealing at 693 K for 40 hours varies from 0 % for sample 1 to 83 % for sample 10.

Similar experiments on twin-roll quenched foils show that the reproducibility is the same for twin-roll quenched foils as for melt-spun ribbons. The variation in thermal stability from sample to sample may be explained by differences in cooling rates, in contamination, or in composition. An effect of composition may occur, due to compositional fluctuations between the $\sim 3g$ alloy pieces

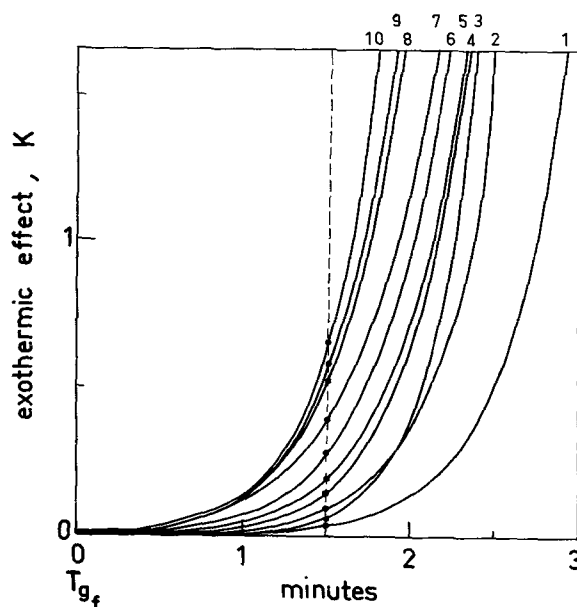


FIG. 1. - Beginning of the crystallization exotherms for ten melt-spun ribbons. All the samples had the same mass (14.5 mg). Time is counted starting from T_{gf} . The heating rate was 10 K.min⁻¹.

chipped from the starting ingot and then used for quenching from the melt. However the study of Kerns (2) on the effect of composition on the thermal characteristics of Cu-Zr amorphous alloys shows that an increase ΔT_c of 20 K corresponds to a change of 4 atomic % Zr. It is unlikely that such inhomogeneities exist in the starting ingot, prepared by levitation melting.

Effect of oxygen contamination.

Effects of surface contamination are readily observed :

- Amorphous $\text{Cu}_{60}\text{Zr}_{40}$ alloys undergo change in surface colour when kept in air for several days.

- The atmosphere in the DTA (pure argon) is not sufficiently clean to prevent oxidation of the amorphous samples during the runs and some "blackening" of the surface is visible to the eye.

These surface effects are accompanied by the occurrence, on the X-ray diffraction pattern, of a narrow diffraction line superimposed on the beginning of the first broad peak characteristic of the amorphous structure. This line (seen at $2\theta \sim 35^\circ$ when Co radiation is used) is due to metastable (cubic or tetragonal) ZrO_2 . After longer annealing times under pure argon, at temperatures well below T_g , this line becomes more intense and a diffraction pattern corresponding to monoclinic ZrO_2 appears, together with the diffraction pattern of Cu. All these lines disappear upon a light polishing of the surface : It only remains the diffraction pattern characteristic of the $\text{Cu}_{60}\text{Zr}_{40}$ amorphous phase.

In order to observe some effect of oxidation on the DTA curves, two amorphous samples were annealed at 413 K for 7 days, one in air and the other in ultra-high vacuum. The corresponding DTA curves are shown on figure 2.

The lower curve, obtained after annealing in air, shows the occurrence of a second exothermic peak. Moreover, a decrease in the temperature of the onset of crystallization and a decrease in $(T_c - T_g)$ are clearly seen : Contamination by annealing in air leads to a decrease in thermal stability. Similar heat-treatments in pure argon induce similar effects on the DTA curves : a second exothermic peak appears and it increases with annealing time.

In their detailed study of the crystallization of amorphous $\text{Cu}_{60}\text{Zr}_{40}$ alloy, Vitek et al. (1) report that samples previously isothermally annealed

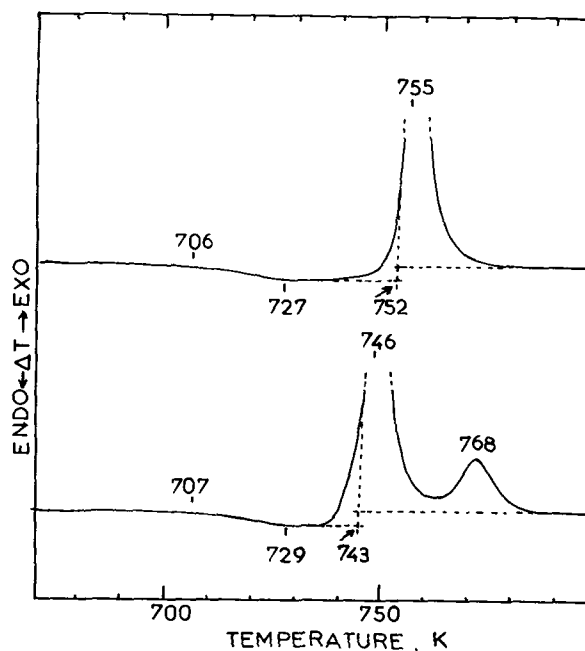


FIG. 2. - DTA curves for amorphous $\text{Cu}_{60}\text{Zr}_{40}$ alloys, after annealing at 413 K for 7 days in ultra-high vacuum (upper curve) or in air (lower curve).

led below the crystallization temperature exhibit two exothermic reactions. As annealing is performed in a DTA under an argon atmosphere, contamination during annealing is suggested. Vitek proposes that the first exothermic peak corresponds to the crystallization of the initial amorphous structure and the second peak corresponds to the crystallization of a "transformed amorphous structure". He follows the annealing behaviour by transmission electron microscopy. When crystallization has been initiated, he finds regions in the foils the electron diffraction pattern of which exhibits two broad halo rings, that corresponding to the initial amorphous matrix and a second one, at a larger d spacing, corresponding to the "transformed amorphous matrix". We have observed our amorphous samples by transmission electron microscopy. Figure 3a) is an electron diffraction pattern of an amorphous foil observed immediately after thinning. This thinned foil was kept in air for three months and observed again. Figure 3b) is the corresponding diffraction pattern : a broad inner halo is seen, at k values corresponding to the (111) reflection of cubic ZrO_2 mentioned above. Thus it is believed that the "transformed amorphous phase" observed by Vitek is an amorphous Cu-Zr phase

rich in oxygen. In the samples studied by Vitek this phase is likely to be formed during annealing in argon.

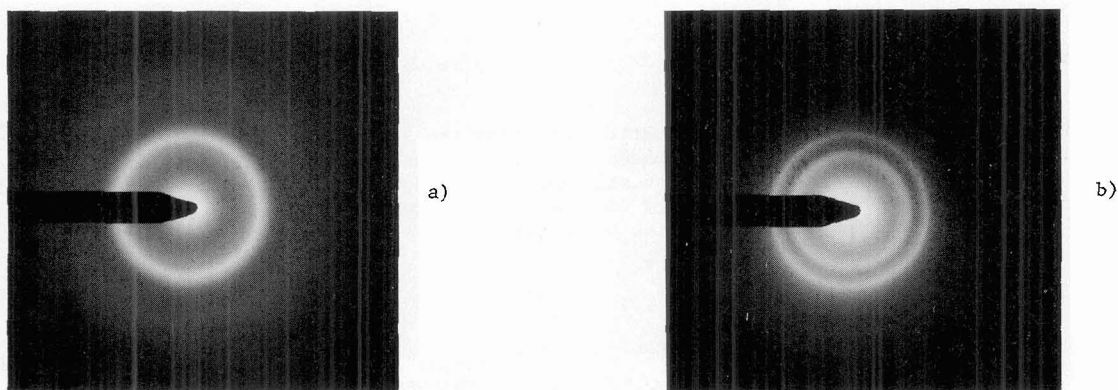


FIG. 3 - Electron diffraction patterns of an amorphous $\text{Cu}_{60}\text{Zr}_{40}$ foil.
a) observed immediately after thinning.
b) kept in air for three months and observed again.

We have followed the behaviour of the DTA curves as a function of previous isothermal annealing in the temperature range 673-713 K studied by Vitek. The heat-treatments were performed in ultra-high vacuum. In these conditions crystallization occurs by a single exothermic reaction. X-ray data show that the equilibrium crystalline phase is formed. Figure 4 illustrates the beginning of crystallization, as detected by X-ray diffraction. The presence of a weak ZrO_2 line is pointed out.

Thus, from this study it appears that very carefully controlled conditions must be achieved for the preparation as for the characterization of amorphous Cu-Zr alloys. In these conditions, amorphous samples prepared by twin-roll quenching or by melt-spinning do not show any significant differences in their thermal behaviour.

References.

- (1) Vitek, J.M., Vander Sande, J.B., and Grant, N.J., Acta Met. 23 (1975) 165.
- (2) Kerns, A.J., Ph.D., Northeastern University (1974).
- (3) Kerns, A.J., Polk, D.E., Ray, R., and Giessen, B.C., Mater. Sci. Eng. 38 (1979) 49.
- (4) Polk, D.E., and Chen, H.S., J. Non-Crystalline Solids 5 (1970) 1.

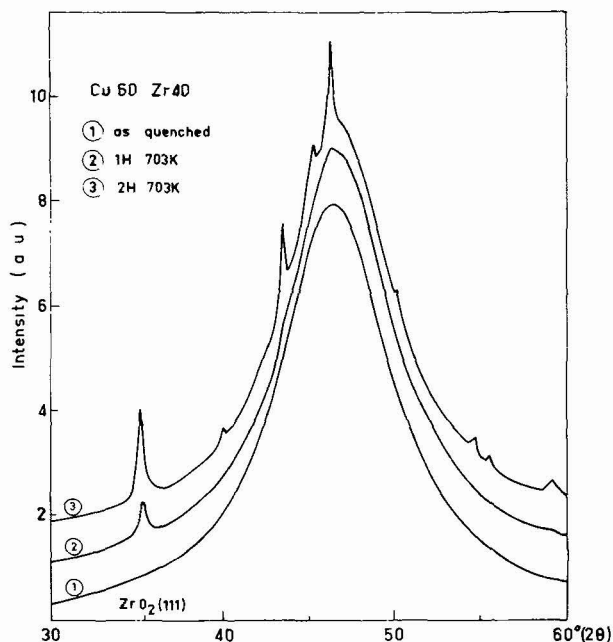


FIG. 4. - X-ray diffraction patterns (Co K α radiation) for a $\text{Cu}_{60}\text{Zr}_{40}$ sample. Curves (2) and (3) are shifted for more clarity. A beginning of crystallization is detected after isothermal annealing at 703 K for 1 hour (curve (2)).